Received: 15 July 2021 | Accepted: 20 January 2022

DOI: 10.1111/1365-2435.14017

Functional Ecology | BRITISH ECOLOGICAL SOCIETY

RESEARCH ARTICLE

Amino acid $\delta^{13}C$ fingerprints of nearshore marine autotrophs are consistent across broad spatiotemporal scales: An intercontinental isotopic dataset and likely biochemical drivers

Emma A. Elliott Smith[1,2] | Michael D. Fox[3,4] | Marilyn L. Fogel[5] | Seth D. Newsome[2]

[1]National Museum of Natural History, Smithsonian Institution, Washington, DC, USA

[2]Department of Biology, University of New Mexico, Albuquerque, NM, USA

[3]Red Sea Research Center, Division of Biological and Environmental Science and Engineering, King Abdullah University of Science and Technology, Thuwal, Saudi Arabia

[4]Woods Hole Oceanographic Institution, Woods Hole, MA, USA

[5]EDGE Institute, University of California – Riverside, Riverside, CA, USA

Correspondence
Emma A. Elliott Smith
Email: ElliottSmithE@si.edu

Funding information
National Science Foundation Graduate Research Fellowship, Grant/Award Number: 1418062

Handling Editor: Zacchaeus Compson

Abstract

1. Carbon isotope fingerprinting, or multivariate analysis using $\delta^{13}C$ values of individual compounds, is a powerful tool in ecological studies, particularly measurements of essential amino acids (EAA $\delta^{13}C$). Despite the widespread application of this technique, there has been little methodological validation to determine (a) whether multivariate EAA $\delta^{13}C$ signatures (fingerprints) of primary producer groups vary across space and time and (b) what biochemical mechanisms drive these patterns.
2. Here, we evaluate the spatiotemporal consistency in EAA $\delta^{13}C$ fingerprints among nearshore primary producers: Chlorophyta (*Ulva* sp.), Ochrophyta (kelps), particulate organic matter (POM) and phytoplankton, and Rhodophyta. We analysed 135 samples from 14 genera collected in Alaska, California and Chile. The collections included historical museum samples (1896–1980 CE) of the giant kelp, *Macrocystis pyrifera*. We employed canonical analysis of principal coordinates and generalized linear models (GLMs) to, respectively, characterize isotopic fingerprints and evaluate the effect of taxonomy, local upwelling regimes, ecological setting, and time on individual EAA $\delta^{13}C$ values and associated fingerprints. We also calculated amino acid discrimination values ($\Delta^{13}C$) to identify key biochemical pathways responsible for these patterns.
3. We found remarkable consistency in EAA $\delta^{13}C$ fingerprints of marine algae across space and through time. Kelps and rhodophytes exhibited statistically distinct multivariate isotopic patterns regardless of geographical location, species identity or time (kelps). In contrast, isotopic fingerprints of POM/phytoplankton and *Ulva* overlapped substantially. GLMs indicated that producer family, presumably due to the presence/absence of carbon concentrating mechanisms, and site locality are important determinants of individual amino acid $\delta^{13}C$ values. Taxonomy was also a key variable for EAA $\delta^{13}C$ fingerprints. The calculated discrimination values suggest variation in (a) metabolism of pyruvate and oxaloacetate-derived amino acids and (b) production of storage and structural carbohydrates are responsible for taxonomic differences in isotopic fingerprints.
4. We conclude EAA $\delta^{13}C$ fingerprinting is a robust method for tracing the contribution of diverse primary producer taxa to coastal food webs. We show that this

technique can be applied to modern and historical samples, as well as consumers collected across continental scales. The high fidelity of EAA $\delta^{13}C$ multivariate patterns coupled with biochemical mechanisms provides a powerful framework for future studies of carbon flow across broad biogeographical and ecological contexts.

KEYWORDS
essential amino acid $\delta^{13}C$ fingerprinting, food webs, kelps, multivariate isotopic patterns, phytoplankton, Rhodophyta, *Ulva*, $\delta^{13}C$

1 | INTRODUCTION

The analysis of stable isotope values within individual compounds has emerged as a powerful tool within the natural sciences (Budge et al., 2008; Close, 2019; Fantle et al., 1999; Fogel & Tuross, 2003; Whiteman et al., 2019). For ecological studies, the carbon isotope composition ($\delta^{13}C$) of individual amino acids holds particular promise for tracing energetic flows within (Howland et al., 2003; Newsome et al., 2014) and among organisms (Fogel & Tuross, 2003; Larsen et al., 2009, 2013). A key advantage of this approach is that variation in the isotopic composition of amino acids can be interpreted within a biochemical framework of synthesis and degradation pathways as these molecules are assimilated by organisms (Whiteman et al., 2019). For example, eukaryotic consumers can readily synthesize or modify 'nonessential' amino acids (NEAA) depending on nutritional requirements, making isotopic analysis of these compounds useful for evaluating animal physiology (Lübcker et al., 2020; Newsome et al., 2014; Whiteman et al., 2020). In contrast, the carbon skeletons of 'essential' amino acids (EAA) are predominantly synthesized by plants, algae and some microbes (Wu, 2009). As a result, eukaryotic consumers typically route EAA from diet, resulting in minimal isotopic alteration with trophic transfers (Fantle et al., 1999; Hare et al., 1991; Howland et al., 2003; McMahon et al., 2015). EAA thus serve as conservative tracers for the sources of primary production fueling food webs.

Many recent compound-specific isotopic studies have relied heavily on a statistical technique known as EAA $\delta^{13}C$ 'fingerprinting'. This work stems from the observation that some primary producer taxa have distinct amino acids $\delta^{13}C$ values (Larsen et al., 2009, 2013; Scott et al., 2006). When viewed in multivariate space via principal component or linear discriminant analysis, these differences can result in statistically evident 'fingerprints' among producer taxa. Scott et al. (2006) first developed this technique to investigate metabolic pathways used by micro-organisms. Subsequent work found that multivariate EAA $\delta^{13}C$ fingerprints also differ among multicellular autotrophs (Larsen et al., 2009), and may be conserved across a range of environmental and laboratory conditions (Larsen et al., 2013, 2015). These autotrophic fingerprints can be identified in consumers and used to characterize the sources of energy supporting individual animals and communities (Elliott Smith et al., 2018, 2021; Fox et al., 2019; Larsen et al., 2013; Rowe et al., 2019). EAA $\delta^{13}C$ fingerprinting has been employed to track animal habitat use and characterize the basal carbon sources supporting arctic, temperate and tropical marine consumers (Arthur et al., 2014; Elliott Smith et al., 2018, 2021; Fox et al., 2019; Rowe et al., 2019); assess linkages among aquatic and terrestrial environments (Jarman et al., 2017; Larsen et al., 2012; Liew et al., 2019; Thorp & Bowes, 2017); and characterize changes in ocean sediment biogeochemical cycles (Larsen et al., 2015).

Despite the many applications of EAA $\delta^{13}C$ fingerprinting, limited research has evaluated the mechanisms driving variability in primary producer amino acid $\delta^{13}C$ values and associated isotopic fingerprints. Notably, we lack information regarding how consistent EAA $\delta^{13}C$ multivariate patterns are within taxonomic units, across localities, and through time (but see Larsen et al., 2013, 2015). By characterizing variation in EAA $\delta^{13}C$ multivariate patterns in response to these factors, we can gain a more comprehensive understanding of how appropriate this technique is over different spatiotemporal scales. Furthermore, apart from the seminal work by Scott et al. (2006), the literature using multivariate isotopic fingerprints has glossed over the biochemical foundations of this technique. It is presumed that differences among taxa in biochemical pathways, or amino acid metabolism, are responsible for the documented EAA $\delta^{13}C$ fingerprints observed to date (Larsen et al., 2009, 2013). However, studies rarely attempt to characterize which pathways or enzymatic reactions are most influential in this regard.

The carbon skeletons of all amino acids are derived from precursors formed during central carbon metabolism (Figure 1; Nelson et al., 2008). The six essential amino acids commonly measured (Silfer et al., 1991) and used in isotopic fingerprinting analyses can be grouped into three precursor families: (a) phosphoenolpyruvate (phenylalanine), (b) pyruvate (leucine and valine) and (c) oxaloacetate (isoleucine, lysine and threonine). The non-essential amino acids alanine and aspartic acid share the same carbon atoms as two of these precursors—pyruvate (Ala) and oxaloacetate (Asp)—and are synthesized via a single reaction involving the addition or removal of an amine group (Kanehisa & Goto, 2000). Alanine and aspartic acid can thus serve as isotopic proxies for important metabolic intermediaries (Scott et al., 2006), and by extension, the differences in $\delta^{13}C$ values between alanine or aspartic acid and downstream amino acids, such as valine or threonine, can provide a metric for the isotopic discrimination associated with that synthesis pathway (Scott et al., 2006). Thus, by examining isotopic variation within and among amino acids—especially those which contribute significantly to multivariate patterns derived from EAA $\delta^{13}C$ data—we can identify key mechanisms driving these isotopic fingerprints.

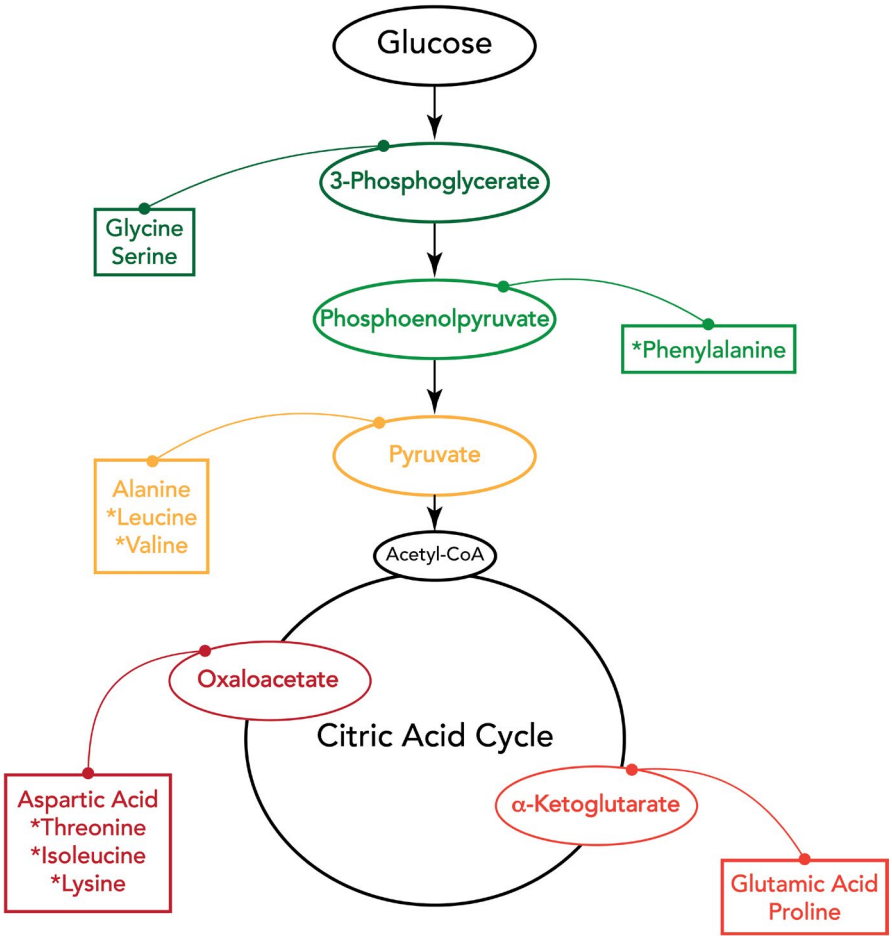

FIGURE 1 Biochemical relationships among amino acids. Shown are the common amino acids reliably measured by CSIA methods, and the intermediaries in central carbon metabolism they are synthesized from. Asterisks (*) indicate amino acids that are considered essential for animals

Here we examine potential environmental and biochemical factors driving variation in amino acid $\delta^{13}C$ values and associated multivariate isotopic fingerprints of nearshore marine autotrophs. We present $\delta^{13}C$ data for 12 amino acids from 135 samples; this is the largest dataset of its kind to date. Our samples span four phyla/functional groups of marine algae collected in Alaska, California and Chile, as well as pure cultures of six phytoplankton genera. In addition, we present data for 13 historical samples of the giant kelp, *Macrocystis pyrifera*, collected from 1896 to 1980 in Monterey Bay, California. We are thus able to evaluate the consistency of multivariate isotopic fingerprints across space and on centennial time-scales. Using this dataset, we explore biogeographical patterns in amino acid $\delta^{13}C$ values and fingerprints and provide likely biochemical mechanisms. Our work represents an important step towards understanding how observed EAA $\delta^{13}C$ multivariate patterns are produced, and the applicability of these analyses across ecological settings.

2 | MATERIALS AND METHODS

2.1 | Sample collection

In total, we analysed 135 samples collected from nearshore sites spanning three oceanographic regions, two continents and 120 years (Table 1). These sites are Katmai National Park, Alaska [58.08°N, 154.47°W; Elliott Smith et al. (2018)], Santa Cruz, California (36.95°N, 122.07°W), San Diego, California (32.86°N, 117.25°W), and Antofagasta, Chile [23.65°S, 70.40°W; Elliott Smith et al. (2021)]. At each site, we collected representative taxa from three phlya of marine macroalgae : Chlorophyta, Ochrophyta and Rhodophyta (Table 1). This included *Ulva* sp., kelps (families Laminariaceae and Lessoniaceae), and understory or intertidal red algae (families Plocamiaceae, Rhodomelaceae, Rhodymeniacea and Gigartinaceae). At every site except for Santa Cruz, we also collected particulate organic matter (POM) of >0.7 μm, a common proxy for phytoplankton. To explore patterns among distinct phytoplankton groups, and evaluate how well isotopic patterns of POM represent those of phytoplankton (Miller & Page, 2012), we sampled pure cultures (one sample each) of red algae (*Porphyridium* sp.), cyanobacteria (*Nodularia* sp.), diatoms (*Amphora* sp., *Chaetoceros* sp., *Phaeodactylum* sp.) and coccolithophores (*Pleurochrysis* sp.) grown at Scripps Institution of Oceanography (La Jolla, CA). Collection details and metadata for all samples are presented in Supporting Information S1.

To determine whether multivariate isotopic patterns can vary within taxa over historical time-scales, we sampled *Macrocystis pyrifera* specimens collected in Monterey Bay from 1896 to 1980. These specimens were dried and preserved on herbarium mounting paper and stored in climate-controlled facilities within the Smithsonian Institution National Museum of Natural History botany collections

TABLE 1 Samples and associated metadata used in the present study

Site	Oceanography	Ecology	Genus	Family	Phylum/Group	N_{AA}^{+} (N_{BULK})	Time Period	CCMs°
Katmai, Alaska	Downwelling	Subtidal	*Saccharina*[•]	Laminariaceae	Ochrophyta	9	Modern	Yes
		Intertidal	*Neorhodomela*	Rhodomelaceae	Rhodophyta	4	Modern	Yes
		Intertidal	*Ulva*	Ulvophyceae	Chlorophyta	5	Modern	Yes
		Surface, offshore	–	–	Particulate organic matter	4	Modern	Yes[*]
Santa Cruz, California	Seasonal Upwelling	Subtidal	*Macrocystis*	Laminariaceae	Ochrophyta	13	Historical	Yes
		Subtidal (drift)	*Macrocystis*	Laminariaceae	Ochrophyta	8	Modern	Yes
		Intertidal	*Neorhodomela*	Rhodomelaceae	Rhodophyta	7	Modern	Yes
		Intertidal	*Ulva*	Ulvophyceae	Chlorophyta	7	Modern	Yes
San Diego, California	Seasonal Upwelling	Subtidal	*Macrocystis*	Laminariaceae	Ochrophyta	15	Modern	Yes
		Subtidal	*Plocamium*	Plocamiaceae	Rhodophyta	6	Modern	No
		Intertidal	*Ulva*	Ulvophyceae	Chlorophyta	5	Modern	Yes
		Surface, nearshore	–	–	Particulate organic matter	7	Modern	Yes[*]
Scripps Institution, California	Cultured	Cultured	*Amphora*	Catenulaceae	Bacillariophyta/Phytoplankton	1	Modern	Yes
		Cultured	*Chaetoceros*	Chaetocerotaceae	Bacillariophyta/Phytoplankton	1 (0)	Modern	Yes
		Cultured	*Nodularia*	Aphanizomenonaceae	Cyanobacteria/Phytoplankton	1 (0)	Modern	Yes
		Cultured	*Phaeodactylum*	Phaeodactylaceae	Bacillariophyta/Phytoplankton	1 (0)	Modern	Yes
		Cultured	*Pleurochrysis*	Syrcosphaeraceae	Haptophyta/Phytoplankton	1	Modern	Yes
		Cultured	*Porphyridium*	Porphyridiaceae	Rhodophyta/Phytoplankton	1 (0)	Modern	Yes
Antofagasta, Chile	Consistent Upwelling	Subtidal	*Lessonia*	Lessoniaceae	Ochrophyta	7	Modern	Yes[†]
		Subtidal	*Macrocystis*	Laminariaceae	Ochrophyta	5 (4)	Modern	Yes
		Subtidal	*Plocamium*	Plocamiaceae	Rhodophyta	4	Modern	No
		Subtidal	*Rhodymenia*	Rhodymeniaceae	Rhodophyta	1	Modern	No
		Subtidal	*Chondrus*	Gigartinaceae	Rhodophyta	1	Modern	Yes
		Subtidal	–	–	Rhodophyta	1	Modern	–
		Intertidal	*Ulva*	Ulvophyceae	Cholorophyta	7	Modern	Yes
		Surface, nearshore & offshore	–	–	Particulate organic matter	13 (11)	Modern	Yes[*]

Notes: Taxonomy from AlgaeBase (Guiry et al., 2014). ([+]) Sample sizes provided are for amino acid $\delta^{13}C$ analysis, number of samples with bulk values provided parenthetically when these samples sizes differ. (°) CCMs = carbon concentrating mechanisms (Badger et al., 1998; Badger & Price, 2003; Reinfelder, 2011; Smith & Bidwell, 1987; Stepien et al., 2016). ([•]) Originally identified as *Laminaria* sp. but confirmed with Alaska USGS in 2021 that this is more likely *Saccharina latissma* following taxonomic reorganization. ([*]) Species identities of POM samples are unknown; however, eukaryotic marine phytoplankton typically possess CCMs. ([†]) The presence of CCMs has been evaluated in other kelps but not this genus.

(Washington, DC). To allow for direct comparison with our modern macroalgae samples, we selected historical kelps collected no more than 50 km from our Santa Cruz sampling locality. From each kelp specimen ($n = 13$), we sampled ~150 mg from non-sporophyll lamina, selecting sections opportunistically to minimize damage to each specimen.

2.2 | Isotopic analysis

Isotopic analyses are reported as δ values in parts per thousand, or per mil (‰), where $\delta^{13}C$ or $\delta^{15}N = 1{,}000 \times [(R_{samp}/R_{std}) - 1]$, and R_{samp} and R_{std} are the ^{13}C: ^{12}C or ^{15}N:^{14}N ratios of the sample and standard. All samples were calibrated against the internationally accepted standards for carbon and nitrogen, respectively, Vienna-Pee Dee Belemnite (V-PDB) and atmospheric N_2. For bulk tissue analysis, macroalgae specimens were rinsed with deionized water, placed in microcentrifuge tubes with perforated caps (1–2 holes), and then lyophilized overnight in a Labconco benchtop freeze dryer at −70°C. Dried algae were then roughly homogenized and sealed in tin capsules (~2–6 mg) for bulk isotope analysis. Pieces of GF/F filters containing POM were lyophilized as above, weighed out to ~10–20 mg and sealed in tin capsules. Bulk tissue $\delta^{13}C$ and $\delta^{15}N$ values, along with weight percent [C] and [N], were measured via EA-IRMS using a Costech 4010 elemental analyzer (Costech) coupled to a Thermo Scientific Delta V Plus isotope ratio mass spectrometer at the University of New Mexico Center for Stable Isotopes (UNM-CSI). Standard deviations of the in-house reference materials (*Bouteloua gracilis* and *Aesculus californica*) were ≤0.2‰ for bulk tissue $\delta^{13}C$ and $\delta^{15}N$ values. We were unable to measure bulk tissue $\delta^{13}C$ and $\delta^{15}N$ values of seven samples due to low peak sizes but retained enough original material for amino acid $\delta^{13}C$ analysis.

For amino acid $\delta^{13}C$ analysis, 5–10 mg of tissue from each sample was hydrolysed in 1 ml, or 1.5 ml (POM), of 6 N hydrochloric acid (110°C, 20 hr); tubes were flushed with N_2 to prevent oxidation. Following hydrolysis, primary producer samples were dried under N_2 gas. 4 ml of 0.01 N HCl was then added to dried hydrolysates and this solution was passed through a cation exchange resin column (Dowex 50WX8 100-200 mesh; Alfa Aesar). This process isolated amino acids from other metabolites, with amino acids eluted using a 2 N ammonium hydroxide solution and dried under N_2 (Amelung & Zhang, 2001). Samples were then derivatized to *N*-trifluoroacetic acid isopropyl esters following established protocols (Silfer et al., 1991). Samples were derivatized in batches ($n = 8$–25) along with an in-house reference material of known isotopic composition containing all 12 amino acids of interest. The derivatizing agents add carbon to the side chains of amino acids, and hence the $\delta^{13}C$ values measured via GC-C-IRMS (see below) reflect a combination of the intrinsic amino acid carbon and reagent carbon. We corrected for this using measured derivative and intrinsic $\delta^{13}C$ values of our in-house reference material; see Supporting Information S2 and Table S1 for details on these corrections.

The $\delta^{13}C$ values of all derivatized amino acids were measured via a GC-C-IRMS system at UNM-CSI. Derivatized samples were injected into a 60 m BPx5 gas chromatograph column (0.32 ID, 1.0μm film thickness, SGE Analytical Science) for amino acid separation within a Thermo Scientific Trace 1310, combusted into CO_2 gas via a coupled Thermo Scientific Isolink II, and analysed with a Thermo Scientific Delta V Plus isotope ratio mass spectrometer. Samples were run in duplicate or triplicate and bracketed with our in-house reference material; we discarded data where standard deviations were >1.2‰ across injections of a sample and report sample means across injections. Daily standard deviations of derivatized amino acid $\delta^{13}C$ values for the in-house reference material ranged from 0.1‰ (isoleucine) to 2.2‰ (serine) but averaged <0.5‰ (Table S1). We report $\delta^{13}C$ values of 12 amino acids, six of which are considered essential—isoleucine (Ile), leucine (Leu), lysine (Lys), phenylalanine (Phe), threonine (Thr) and valine (Val), and six nonessential—alanine (Ala), aspartic acid/asparagine (Asp), glutamic acid/glutamine (Glu), glycine (Gly), proline (Pro) and serine (Ser). For 14 of our total 135 samples, we were not able to obtain reliable $\delta^{13}C$ values for either one or two amino acids: Pro ($n = 4$), Gly ($n = 4$), Ser ($n = 2$; one of these samples was also missing Gly), Asp ($n = 1$), Glu ($n = 1$), and Phe ($n = 2$) and Lys ($n = 1$). We excluded these samples as necessary for subsequent analyses.

2.3 | Statistical analyses

Our isotopic data failed assumptions of multivariate and univariate normality due to rhodophytes with low bulk tissue and amino acid $\delta^{13}C$ values (Table S2). Thus, to evaluate the factors driving compound-level variation in marine algae isotopic values, we conducted a series of nonparametric tests to (a) evaluate broad differences among taxa/sites, (b) assess the relative influence of environmental and physiological factors on amino acid $\delta^{13}C$ values and (c) characterize EAA $\delta^{13}C$ multivariate patterns (fingerprints). We also computed differences in $\delta^{13}C$ values among biochemically related amino acids and evaluated whether these discrimination values ($\Delta^{13}C$) varied among groups. All analyses were run in R [v4.0.3; (R Development Core Team, 2020)] with RStudio interface (v1.1.463).

We used Kruskal–Wallis and Wilcoxon signed-rank tests to assess differences in bulk tissue $\delta^{13}C$ and $\delta^{15}N$ values among sites for each primary producer group (kelps, red algae, green algae and POM); pure phytoplankton cultures were excluded from this analysis due to low sample size ($n = 2$). We then explored whether there were differences among primary producers (across all sites) in amino acid $\delta^{13}C$ values using Wilcoxon signed-rank tests. These latter analyses indicated that cultured Scripps phytoplankton and POM samples were isotopically similar (Table S4), and we pooled data from these groups in all subsequent analyses (GLMs, CAP).

Following these tests, we employed generalized linear models (GLMs) to determine the most influential predictors of amino acid $\delta^{13}C$ values (Tables S5 and S6). For each amino acid, we compared alternative models within an information theoretic framework (Aho

et al., 2014; Burnham & Anderson, 2002, 2004), evaluating relative support for models with combinations of the following main effects: presence/absence of carbon concentrating mechanisms (CCMs), taxonomic identity (phylum, with POM/phytoplankton considered together, and family), site locality, oceanographic conditions (downwelling, seasonal upwelling, consistent upwelling) and ecological setting (intertidal, subtidal, surface nearshore, surface offshore or cultured). We considered interaction effects between family and site, as well as family and ecological setting. In all cases, we also evaluated support for a constant model with no effects or interactions and considered the model with the lowest Akaike information criterion (AIC) score the best supported model for a response variable.

We first conducted GLMs on the full dataset, excluding two red algae genera for which we only had a single datapoint, and one red algae sample without a definitive taxonomic identification. In addition, we conducted separate GLMs for each phylum/group (POM & phytoplankton considered together) to see whether the same or different factors influence amino acid $\delta^{13}C$ values of marine autotroph as a whole compared to specific taxa; for kelps, we included an additional effect of time (historical vs. modern). Tables S5 and S6 present AIC, log-likelihood and number of parameters for all GLM models.

To characterize amino acid $\delta^{13}C$ multivariate patterns, or fingerprints, we used canonical analysis of principal coordinates, or CAP (Anderson & Willis, 2003), which has been employed successfully with EAA $\delta^{13}C$ data (Elliott Smith et al., 2018). We ran two CAP models. The first, henceforth termed 'CAP_{ALL}', included all 12 measured amino acids. The second model, 'CAP_{EAA},' included only those considered essential for animals (Ile, Leu, Lys, Phe, Thr and Val). Both models were run using a Euclidean distance matrix with un-normalized data and 999 permutations. We used a leave-one-out and cross-validation procedure to obtain group-specific classification error rates for POM/phytoplankton, green algae, red algae and kelps, to assess whether these groups are statistically distinct in their isotopic multivariate patterns. We calculated *post hoc* product–moment correlations between each original variable (amino acid $\delta^{13}C$ values) and the two primary canonical axes to determine which amino acids were most influential in determining the isotopic fingerprints (Anderson & Willis, 2003). Finally, to assess whether the same or different factors drive isotopic multivariate patterns as individual amino acid $\delta^{13}C$ values, we evaluated the coordinates of each sample along canonical axes 1 and 2 (CAP_{EAA} model) in the GLM framework described above; we conducted this analysis only for the full dataset.

After characterizing amino acid $\delta^{13}C$ multivariate patterns, we aimed to provide a more mechanistic biochemical framework to explain these patterns. Expanding from the seminal work by Scott et al. (2006), we compared $\delta^{13}C$ values of amino acids derived from the same precursor, or synthesized from one another (e.g. isoleucine from threonine). These differences in $\delta^{13}C$ values among amino acid pairs provide a metric for the isotopic discrimination associated with a given synthesis pathway. We used the KEGG Pathway database to define synthesis pathways (Kanehisa & Goto, 2000). We relied on the reference maps as only two of our sampled genera (*Chondrus* and *Phaeodactylum*) are included in KEGG. For each phylum (POM/phytoplankton considered together as a 'phylum'), we calculated the following discrimination values ($\Delta^{13}C = \delta^{13}C_{product} - \delta^{13}C_{precursor}$) based on the most influential amino acids in both CAP models (Tables S7 and S8): $\Delta^{13}C_{Val\text{-}Ala}$, $\Delta^{13}C_{Thr\text{-}Asp}$, $\Delta^{13}C_{Ile\text{-}Asp}$, $\Delta^{13}C_{Ile\text{-}Thr}$, $\Delta^{13}C_{Lys\text{-}Asp}$ and $\Delta^{13}C_{Pro\text{-}Glu}$; alanine serves as a proxy for pyruvate (Scott et al., 2006). We also calculated $\Delta^{13}C_{Ser\text{-}Gly}$ to serve as a 'null' model, as these amino acids were not important for isotopic multivariate patterns (Table S7). We calculated $\Delta^{13}C$ for each sample and then took the phylum average. We tested for group-level differences using Wilcoxon signed-rank tests.

3 | RESULTS

3.1 | Isotopic composition of marine producers

Bulk tissue and amino acid isotope values varied among nearshore primary producer groups and localities (Figure 2; Tables S3 and S4). Bulk tissue $\delta^{15}N$ values differed among sites (Kruskal–Wallis: $\chi^2 = 74.81$, $p < 0.01$), with algae in Chile having the highest $\delta^{15}N$ and those in Alaska the lowest. Bulk $\delta^{13}C$ values varied among producer taxa ($\chi^2 = 38.68$, $p < 0.01$), with *Ulva* having the highest, and red algae the lowest values (Figure 2; Table S3). We also found differences in amino acids $\delta^{13}C$ values among primary producer clades. Every phylum (and POM/phytoplankton) were statistically distinct from one another for at least two amino acids. Cultured phytoplankton from Scripps differed only marginally from POM samples (all sites) for three amino acids: Leu, Gly and Ser (Table S4).

3.2 | Predictors of amino acid $\delta^{13}C$ values

Considering first the GLMs conducted with the full dataset: for all amino acids measured, we found the strongest support for a model with main effects of primary producer family and collection locality, as well as an interaction effect between these two variables (Table S5). We did not find significant support for our selected ecological or oceanographic variables as predictors of amino acid $\delta^{13}C$ values. Including an effect of ecological setting (intertidal, subtidal, surface nearshore, surface offshore and cultured) and site upwelling regime (downwelling, seasonal or consistent) resulted in extremely poor model performance, with Akaike information criterion (AIC) scores in some cases greater than the null. Taxonomy was clearly an important variable in determining amino acid $\delta^{13}C$ values, but this factor was more informative when broken down at the level of family rather than phylum (Table S5).

We found similar results when conducting GLMs for each primary producer phylum/group independently (Table S6). For red algae, the best supported models included collection locality, or family as predictors of amino acid $\delta^{13}C$ values. For kelps, a model with only a main effect of locality was the best supported, though models including

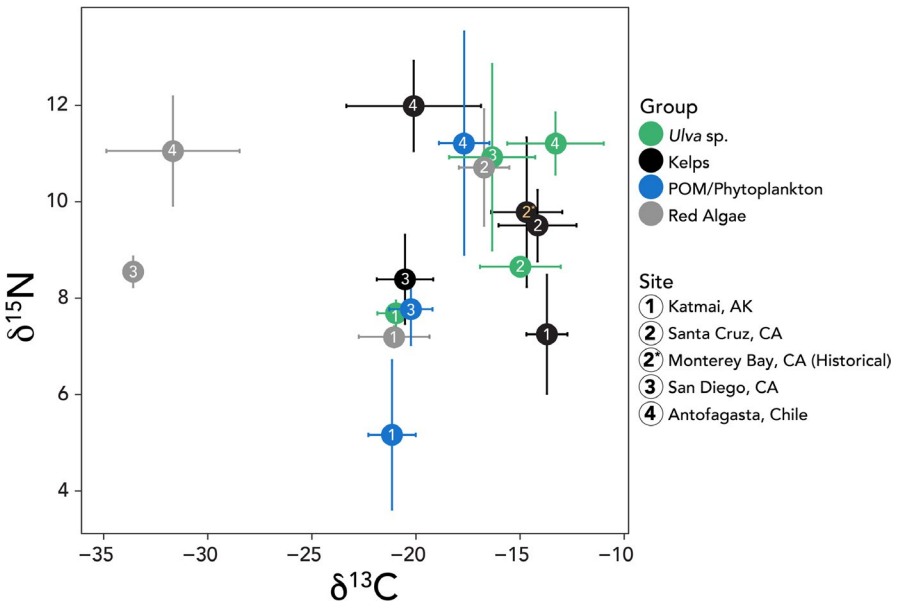

FIGURE 2 Average (±*SD*) bulk $\delta^{13}C$ and $\delta^{15}N$ values for sampled marine autotrophs. Colours represent different primary producer taxa sampled; numbers indicate the locality. See Table 1 for sample sizes and details on collection and specific taxa included. Phytoplankton cultures from Scripps are omitted from this graph due to low sample size for bulk tissue isotopic analysis ($n = 2$)

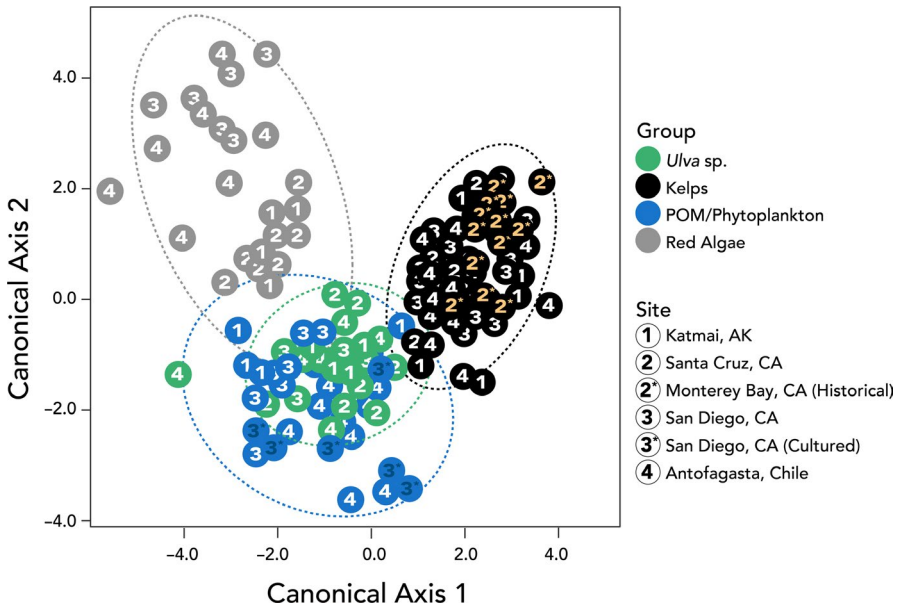

FIGURE 3 Results from canonical analysis of principle coordinates using essential amino acid $\delta^{13}C$ data of marine autotrophs. Circles represent the loading of individual primary producer samples along the first two canonical axes; ellipses surrounding producer groups represent 90% confidence intervals. Carbon isotope values for isoleucine, leucine, lysine, phenylalanine, threonine and valine were used in this analysis; see Table S8 for product–moment correlations of essential amino acid $\delta^{13}C$ values with CAP axes. Colours represent producer taxonomy: Rhodophyta, Ochrophyta, Chlorophyta and particulate organic matter (POM)/phytoplankton. Numbers indicate the locality where each sample was collected. See Table 2 for reclassification rates among primary producer groups

an effect of kelp family were only marginally less supported in some cases (Table S6). We did not find evidence that a temporal effect (historical vs. modern) was important for any kelp amino acid $\delta^{13}C$ values. Green algae (*Ulva* sp.) and POM/cultured phytoplankton showed marginal variation in amino acid $\delta^{13}C$ values among sites, upwelling regimes and—for POM/phytoplankton—nearshore, offshore and cultured samples (Table S6). Parameter estimates and standard errors for all best supported models are presented in the Supporting Information (Table S10).

3.3 | Canonical analysis of principal coordinates—amino acid $\delta^{13}C$ fingerprinting

Results from our multivariate analysis of amino acid $\delta^{13}C$ values showed strong separation among producer groups (Figure 3; Table 2; Figures S7 and S8). For both CAP models, the first two canonical axes (CA) cumulatively explained >95% of the variation in our dataset. For the CAP_{ALL} model, the amino acids that were the most informative for distinguishing among groups were predominantly from the pyruvate and oxaloacetate

TABLE 2 Results from canonical analysis of principal coordinates (CAP) of marine primary producer phyla. Columns represent classification of a sample group as given by CAP; rows represent the group being classified. The cross diagonal (bold text) are correct reclassifications (CAP_{ALL}: 81.0%, CAP_{EAA}: 84.1% across all groups). Numbers falling off this diagonal indicate samples that were incorrectly reclassified by the model. Chlorophyta = Ulva sp., POM = particulate organic matter and cultured Scripps phytoplankton, Ochrophyta (Kelps) = *Lessonia* sp., *Macrocystis pyrifera*, and *Saccharina latissima*, Rhodophyta = Neorhodomela sp., *Plocamium* sp., and singletons of *Chondrus canaliculatus*, *Rhodymenia corallina*, and an unidentified red alga

	CAP classification				
	Chlorophyta	**Ochrophyta (Kelps)**	**POM**	**Rhodophyta**	**% Correct**
CAP_{ALL}: True Producer Identity					
Chlorophyta	**12**	0	9	0	57.1
Ochrophyta (Kelps)	1	**51**	0	0	98.1
POM	7	0	**20**	1	71.4
Rhodophyta	5	0	0	**15**	75.0
CAP_{EAA}: True Producer Identity					
Chlorophyta	**15**	0	8	0	65.2
Ochrophyta (Kelps)	2	**54**	0	0	96.4
POM	9	1	**19**	0	65.5
Rhodophyta	1	0	0	**23**	95.8

families: threonine, valine and aspartic acid were most strongly correlated with CA1, and isoleucine, glutamic acid, and alanine with CA2 (Table S7). We found similar results with the CAP_{EAA} model: threonine, valine and lysine exhibited the strongest correlations with CA1, and isoleucine, lysine, and phenylalanine for CA2 (Table S8). Cross-validation found a high successful reclassification rate among our primary producer phyla/groups for both the CAP_{ALL} (81.0%) and CAP_{EAA} (84.1%) models (Table 2). In both models, this result was significant across permutations. Kelps had the highest successful reclassification rates (CAP_{ALL}: 98.1%, CAP_{EAA}: 96.4%) with only 2 of 56 samples classifying incorrectly with the CAP_{EAA} model. Green algae (*Ulva* sp.) had the lowest successful reclassification rates (CAP_{ALL}: 57.1%, CAP_{EAA}: 65.2%), with samples misclassifying predominantly with POM/phytoplankton. POM/phytoplankton reclassification rates also differed among models (CAP_{ALL}: 71.4%, CAP_{EAA}: 65.5%) with most misclassifications with *Ulva*. Red algae had relatively high reclassification rates in both models with 15/20 (CAP_{ALL}: 75%) and 23/24 (CAP_{EAA}: 95.8%) samples correctly reclassifying. We also examined which factors best predicted the isotopic multivariate patterns derived from CAP using GLM. For variation along the first axis (CA1), the best supported model included main effects of primary producer family and ecology, as well as an interaction effect; a model with only a main effect of family was also supported (Table S5). For CA2, the two best supported models included main and interaction effects of family and locality, or family and ecology (Table S5).

3.4 | Amino acid synthesis and carbon isotope discrimination

We found differences within and among marine primary producers in the isotopic discrimination between product and precursor amino acids (Figure 4; Table S9). The largest $\Delta^{13}C$ was between values of isoleucine and threonine in kelps, with Thr having higher $\delta^{13}C$ values by an average of 12.3‰ ± 2.3‰. The smallest discriminations were in $\Delta^{13}C_{Pro\text{-}Glu}$, ranging from 1.2‰ ± 3.4‰ (kelps) to 0.5‰ ± 1.9‰ (*Ulva*). $\Delta^{13}C_{Ser\text{-}Gly}$ values varied widely, with standard deviations of 6.1‰ (kelps) to 8.1‰ (*Ulva*). Kelps and red algae showed the most unique discriminations, and POM and green algae differed only in $\Delta^{13}C_{Thr\text{-}Asp}$ and $\Delta^{13}C_{Ile\text{-}Asp}$.

4 | DISCUSSION

We found remarkable consistencies in the amino acid isotopic fingerprints of marine primary producer taxa over space and time. Our results indicate that while $\delta^{13}C$ values of individual amino acids vary to some degree based on locality, producer taxonomy was a key factor for determining both amino acid $\delta^{13}C$ and multivariate isotopic patterns (fingerprints). We observed distinct and spatially consistent fingerprints of macroscopic Rhodophyta and Ochrophyta (kelps), suggesting these groups can be reliably identified across broad biogeographical scales. In contrast, we were unable to distinguish particulate organic matter (POM) and phytoplankton from green algae, which presents a limitation in using amino acid $\delta^{13}C$ analysis for characterizing the importance of benthic and pelagic endmembers in some scenarios. Below, we discuss these findings in more detail, and identify several key biochemical pathways that may be driving these patterns. Our study provides a much-needed framework for interpreting primary producer EAA $\delta^{13}C$ multivariate patterns and evaluating the efficacy of the fingerprinting technique across spatiotemporal scales and ecological contexts.

4.1 | Biogeographical patterns of marine primary producer fingerprints

The amino acid $\delta^{13}C$ multivariate patterns (fingerprints) of nearshore marine primary producers were consistent within

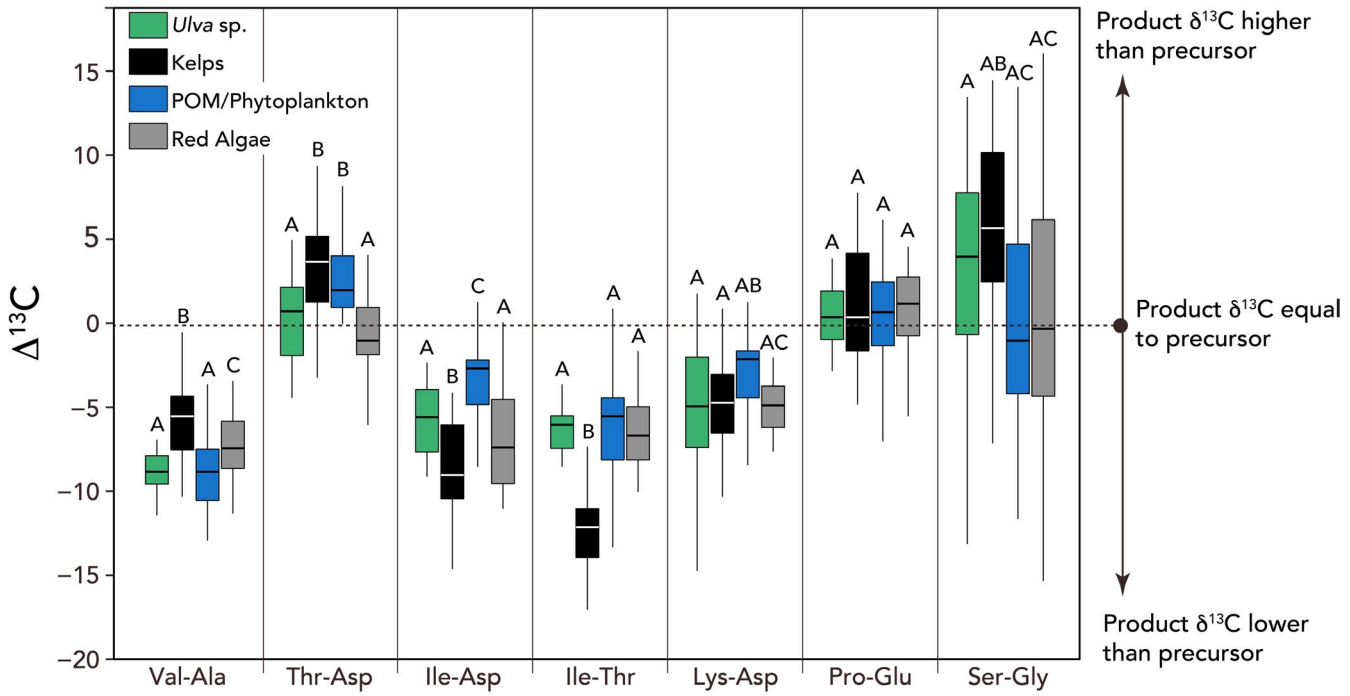

FIGURE 4 Isotopic discrimination among amino acids in marine primary producers. Shown are the isotopic discrimination values between key amino acid pairs representing biochemical pathways that are critical in determining multivariate isotopic fingerprints (see Tables S7 and S8). We compared these data with the isotopic offset between the relatively uninformative amino acids Ser-Gly. Isotopic discrimination values were calculated as $\Delta^{13}C = \delta^{13}C_{Product} - \delta^{13}C_{Precursor}$. Values of 0 thus represent pathways with no measurable discrimination. Boxes represent the spread of data around the median, colours represent different taxonomic groupings and letters indicate statistical groupings for each amino acid pair (see Table S9). Broadly, kelps and red algae show the greatest number of significantly different offsets from other groups

groups across broad spatiotemporal scales. For both the CAP_{ALL} and CAP_{EAA} models, we obtained overall successful reclassification rates of >80% (Figure 3; Table 2). This finding shows the stability and importance of biochemical pathways in setting isotopic fingerprints, as our dataset includes 14 genera collected from two continents over the past 120 years (Table 1), and yet time period was not a key predictor for algae samples in multivariate isotopic space (Table S6). Amino acid $\delta^{13}C$ fingerprints of red algae and kelps were particularly distinct, with 75%–98% of individuals from each group successfully reclassifying in both CAP models (Figure 3; Table 2). This included historical *Macrocystis* samples dating back to 1896 CE, which exhibited the same patterns in amino acid $\delta^{13}C$ values as modern *Macrocystis* (Figure 3). Hence, EAA $\delta^{13}C$ fingerprinting provides a way of tracing the importance of different algal groups, and especially kelp-derived energy, to consumers across both space and time. This technique improves greatly on traditional bulk tissue isotopic analysis, which does not allow for separation among primary producer clades in many localities (Figure 2) and requires consumer-specific trophic discriminations for food web studies (Caut et al., 2009). These findings also highlight the critical role of museum collections in ecological and isotopic research (Miller et al., 2020): the incorporation of historical specimens allowed us to add a temporal perspective, and thus broaden the potential applications of this tool to the fields of historical ecology and perhaps archaeology.

In contrast to the distinct multivariate isotopic patterns of kelps and red algae, we were unable to discriminate between POM/phytoplankton and green algae (*Ulva* sp.). In both CAP models, these groups overlapped substantially (Table 2). For the CAP_{EAA} model, <66% of POM and *Ulva* samples reclassified successfully (Figure 3). This overlap in multivariate space is likely due to broad similarities in biochemical pathways among these groups, and thus similar amino acid $\delta^{13}C$ fingerprints. Notably, the isotopic discrimination values $\Delta^{13}C_{Val\text{-}Ala}$, $\Delta^{13}C_{Ile\text{-}Thr}$ and $\Delta^{13}C_{Lys\text{-}Asp}$ were similar among POM/phytoplankton and *Ulva* (Figure 4), which corresponds to synthesis pathways of amino acids that are important drivers of multivariate isotopic fingerprints (Tables S7 and S8). These results suggest that the biosynthetic pathways of phytoplankton and *Ulva* are too similar to be distinguished among using EAA $\delta^{13}C$ fingerprinting at broad spatial scales, a finding in line with previous work on this topic at local scales and perhaps related to the simplistic morphology of *Ulva* (Elliott Smith et al., 2018; Elliott Smith et al., 2021). It remains to be seen whether this multivariate isotopic overlap is specific to *Ulva* and our sampled POM, or whether this is a broader pattern among green algae and phytoplankton taxa.

4.2 | Physiological and biochemical mechanisms

To better understand primary producer isotopic patterns, we tested which environmental and physiological factors had the greatest

influence on individual amino acid $\delta^{13}C$ values. We found the strongest support for GLMs which predicted $\delta^{13}C$ values from primary producer taxonomy (family), sampling location and an interaction between these two main effects (Table S5). A key determinant in the distinction we found among algae families is likely the presence or absence of carbon concentrating mechanisms (CCMs). Decades of work have determined the mode of inorganic carbon acquisition is a predictor of marine primary producer bulk tissue $\delta^{13}C$ values (Maberly et al., 1992; Raven et al., 2002). In algae, CCMs primarily involve the uptake of HCO_3^-, either directly through an anion transport protein or indirectly through methods such as the production of extracellular carbonic anhydrase (Giordano et al., 2005). The $\delta^{13}C$ values of HCO_3^- and aqueous CO_2 are distinct due to a large equilibrium isotope fractionation ($\Delta^{13}C_{HCO3\text{-}CO2}$ = 9.4‰ at 14°C; Wendt, 1968), and are reflected in the species utilizing these inorganic carbon sources: algae with CCMs have higher bulk tissue $\delta^{13}C$ values in comparison to co-occurring algae that rely exclusively on diffusive CO_2 entry (Maberly et al., 1992; Stepien et al., 2016). Thus, as excepted, our sampled algae lacking CCMs (*Plocamium* and *Rhodymenia*) had the lowest bulk tissue and amino acid $\delta^{13}C$ values, compared to kelps, *Ulva* and POM/phytoplankton (Tables S3 and S4).

Among algae with CCMs, an interaction between taxonomic identity and producer functional group appeared to determine amino acid $\delta^{13}C$ values and multivariate isotopic patterns. Notably, four of the cultured phytoplankton we sampled are within, or closely related to, two of our macroalgae phyla (e.g. the unicellular red alga *Porphyridium*, and three diatoms; Table 1), and yet these samples showed amino acid $\delta^{13}C$ values and isotopic fingerprints consistent with POM samples. This suggests that phylum-level categorizations used for isotopic fingerprinting (Figure 3) may in some cases be less informative than functional groupings (e.g. micro vs. macroalgae). Indeed, our GLM comparison indicated that a taxonomic factor at the level of family was more informative than a phylum classification for predicting amino acid $\delta^{13}C$ values and CA loadings (Tables S5 and S6). However, previous studies have found distinct amino acid $\delta^{13}C$ fingerprints between symbiotic microalgae in corals (Symbiodiniaceae) and local POM (Fox et al., 2019), raising the question of whether such differences among microalgae clades may be observed in other nearshore systems with greater sample size. This highlights the need for additional sampling and analysis of POM and planktonic taxa from coastal ecosystems around the globe.

At the biochemical level, we found taxonomic differences among marine algae in isotopic fingerprints were driven by pyruvate and oxaloacetate-derived amino acid metabolism. Both CAP models found threonine and valine $\delta^{13}C$ values to be highly influential in separating producer groups in multivariate isotopic space, followed by lysine and isoleucine (CAP_{EAA}), or aspartic acid and isoleucine (CAP_{ALL}; Tables S6 and S7). These amino acids are synthesized from pyruvate or oxaloacetate (Figure 1), which directly implicates enzymatic reactions in these pathways as determinants for isotopic fingerprints. This is also evident in the calculated isotopic discriminations, as mean $\Delta^{13}C_{Val\text{-}Ala}$, $\Delta^{13}C_{Thr\text{-}Asp}$ and $\Delta^{13}C_{Ile\text{-}Thr}$ differed significantly among groups, with kelps having lower $\Delta^{13}C_{Ile\text{-}Thr}$ and higher $\Delta^{13}C_{Thr\text{-}Asp}$ and $\Delta^{13}C_{Val\text{-}Ala}$ values (Figure 4). There are several biochemical mechanisms which may result in these differences. First, there may be differences in the structure, or identity, of enzymes participating in amino acid synthesis among groups. Enzymes vary widely in their isotope effects (e.g. Rubisco vs. PEPC; Fogel & Cifuentes, 1993; O'Leary, 1988), and thus divergent enzymatic usage among marine algae clades could very well have imparted distinct multivariate isotopic fingerprints. The most likely culprits are those that catalyse the addition or removal of carbon atoms. Notable examples here include *acetolactate synthase*, which decarboxylates pyruvate to form key precursors in the biosynthesis of valine and isoleucine, and *aspartate-semialdehyde hydrolase*, which catalyses a reaction between aspartate 4-semialdehyde and pyruvate involving the net exchange of three carbon atoms as part of lysine synthesis (Kanehisa & Goto, 2000). At present, taxon-specific data regarding the enzymes participating in amino acid biosynthesis is lacking for many marine macroalgae (Kanehisa & Goto, 2000), and more research is needed into this line of inquiry.

Alternatively, variation in metabolic demands for amino acids may be driving differential fractionation among producer groups to create the observed isotopic fingerprints. Studies of amino acid $\delta^{15}N$ values in terrestrial plants show that increased need for lignin, which is derived from the amino acid phenylalanine, can result in an isotopically heavier pool of Phe used for tissue synthesis (Kendall et al., 2019). Similar mechanisms may be operating in marine algae, which produce a broad array of secondary metabolites in response to biotic and environmental pressures (Norris & Fenical, 1982). Alkaloids, for example, are common in marine algae and are produced through catabolism of aromatic amino acids (Güven et al., 2010; Maschek & Baker, 2008). In addition, marine algae vary in their production of other metabolic compounds. Brown algae, and kelps in particular, produce extremely high levels of the storage/structural polysaccharides mannitol and alginate, which can comprise >40% of kelp tissue by dry weight (Honya et al., 1993). In kelps, both compounds are synthesized from fructose-6-phosphate (Ye et al., 2015; Zhang et al., 2020), which, in turn, may be synthesized from pyruvate or oxaloacetate via gluconeogenesis (Kanehisa & Goto, 2000; Shao et al., 2019). This catabolic process could well have an associated isotope effect that would 'label' amino acids synthesized from the remaining oxaloacetate and pyruvate pools. Furthermore, glucogenic amino acids, including threonine, valine and isoleucine, can be catabolized for gluconeogenesis (Nelson et al., 2008), which may impart further isotope effects. A combination of these processes would explain the distinct isotopic fingerprints we observed here for kelps relative to other macroalgae, as well as the separation between kelps and our sampled diatoms (e.g. *Phaeodactylum*) in multivariate isotopic space (Figure 3). Diatoms do not require the same quantities of structural/storage carbohydrates as kelps, and thus exhibited multivariate isotopic patterns more similar to POM and phytoplankton than to macroscopic brown algae. This mechanism could

be tested in future research by comparing the concentrations of mannitol and alginate within kelp tissues to the $\delta^{13}C$ values of aspartic acid, alanine, threonine, isoleucine and valine.

5 | CONCLUSIONS

Our study combines a biogeographical with a biochemical perspective to understand compound-level isotopic variation and the potential applications of these measurements in characterizing ecological phenomena. Through this work we conclude the following: (a) amino acid $\delta^{13}C$ values of nearshore primary producer taxa are determined by a combination of taxonomy (likely driven by inorganic carbon acquisition strategies) and local environment, (b) amino acid $\delta^{13}C$ multivariate patterns (fingerprints) of these groups are relatively insensitive to spatial and temporal variation and (c) there are a small number of key molecules and biochemical pathways that are likely responsible for these patterns and warrant further investigation. EAA $\delta^{13}C$ fingerprinting thus provides researchers with a high-resolution method of tracing the flow of energy through various compartments of nearshore subtidal and intertidal food webs, as well as adjacent terrestrial and pelagic ecosystems. One of the most powerful applications for EAA $\delta^{13}C$ fingerprinting is studying historical and archaeological specimens, which will allow researchers to assess how vulnerable communities were structured in pre-colonial/pre-industrial time periods, and how they have responded to environmental change. Our study exemplifies the powerful utility of isotopic analysis of individual compounds in characterizing ecological patterns and dynamics across space and time.

ACKNOWLEDGEMENTS

We would like to express our gratitude to James Norris and Torrey Rick for their time and assistance in sampling the historical kelps presented in this manuscript. We would also like to thank Laura Burkemper and Viorel Atudorei for their laboratory expertise and boundless support throughout this project. Thanks to Peter Raimondi, Maya George, Monica Moritsch, Kelton McMahon and Sarah Foster for facilitating/assisting in macroalgae sampling in California, and Orna Cook for providing phytoplankton cultures. A special thank you to Rosemary Elliott Smith for statistical consulting and general support. We also greatly appreciate the constructive feedback on this work provided by Joe Cook, Tom Turner, Jim Estes and Torrey Rick. E.A.E.S. was supported by NSF (GRFP-1418062), as well as the UNM Latin American Iberian Institute, Department of Biology, and UNM-CSI.

CONFLICT OF INTEREST

The authors declare they have no conflicts of interest.

AUTHORS' CONTRIBUTIONS

E.A.E.S. and S.D.N. conceived the ideas and designed the methodology with input from M.L.F.; E.A.E.S. collected the data with field assistance from M.D.F.; E.A.E.S. wrote the manuscript, and all authors contributed critically to the drafts and gave approval for publication.

DATA AVAILABILITY STATEMENT

Data deposited in the Dryad Digital Repository https://doi.org/10.5061/dryad.zw3r22897 (Elliott Smith et al., 2022).

ORCID

Emma A. Elliott Smith https://orcid.org/0000-0002-3221-0737
Michael D. Fox https://orcid.org/0000-0002-5004-1025
Seth D. Newsome https://orcid.org/0000-0002-4534-1242

REFERENCES

Aho, K., Derryberry, D., & Peterson, T. (2014). Model selection for ecologists: The worldviews of AIC and BIC. *Ecology*, *95*, 631–636. https://doi.org/10.1890/13-1452.1

Amelung, W., & Zhang, X. (2001). Determination of amino acid enantiomers in soils. *Soil Biology and Biochemistry*, *33*(4–5), 553–562.

Anderson, M. J., & Willis, T. J. (2003). Canonical analysis of principal coordinates: A useful method of constrained ordination for ecology. *Ecology*, *84*(2), 511–525.

Arthur, K. E., Kelez, S., Larsen, T., Choy, C. A., & Popp, B. N. (2014). Tracing the biosynthetic source of essential amino acids in marine turtles using $\delta^{13}C$ fingerprints. *Ecology*, *95*, 1285–1293.

Badger, M. R., Andrews, T. J., Whitney, S., Ludwig, M., Yellowlees, D. C., Leggat, W., & Price, G. D. (1998). The diversity and coevolution of Rubisco, plastids, pyrenoids, and chloroplast-based CO_2-concentrating mechanisms in algae. *Canadian Journal of Botany*, *76*, 1052–1071.

Badger, M. R., & Price, G. D. (2003). CO_2 concentrating mechanisms in cyanobacteria: Molecular components, their diversity and evolution. *Journal of Experimental Botany*, *54*, 609–622. https://doi.org/10.1093/jxb/erg076

Budge, S., Wooller, M., Springer, A., Iverson, S. J., McRoy, C., & Divoky, G. (2008). Tracing carbon flow in an arctic marine food web using fatty acid-stable isotope analysis. *Oecologia*, *157*, 117–129. https://doi.org/10.1007/s00442-008-1053-7

Burnham, K. P., & Anderson, D. R. (2002). *Model selection and multimodel inference: A practical information-theoretic approach* (Vol. 2). Springer.

Burnham, K. P., & Anderson, D. R. (2004). Multimodel inference: Understanding AIC and BIC in model selection. *Sociological Methods & Research*, *33*, 261–304. https://doi.org/10.1177/0049124104268644

Caut, S., Angulo, E., & Courchamp, F. (2009). Variation in discrimination factors ($\Delta^{15}N$ and $\Delta^{13}C$): The effect of diet isotopic values and applications for diet reconstruction. *Journal of Applied Ecology*, *46*, 443–453.

Close, H. G. (2019). Compound-specific isotope geochemistry in the ocean. *Annual Review of Marine Science*, *11*, 27–56. https://doi.org/10.1146/annurev-marine-121916-063634

Elliott Smith, E. A., Fox, M. D., Fogel, M. L., & Newsome, S. D. (2022). Data from: Amino acid $\delta^{13}C$ dataset for nearshore marine primary producers. *Dryad Digital Repository*, https://doi.org/10.5061/dryad.zw3r22897

Elliott Smith, E. A., Harrod, C., Docmac, F., & Newsome, S. D. (2021). Intraspecific variation and energy channel coupling within a Chilean kelp forest. *Ecology*, *102*, e03198.

Elliott Smith, E. A., Harrod, C., & Newsome, S. D. (2018). The importance of kelp to an intertidal ecosystem varies by trophic level: Insights from amino acid $\delta^{13}C$ analysis. *Ecosphere*, *9*, e02516.

Fantle, M. S., Dittel, A. I., Schwalm, S. M., Epifanio, C. E., & Fogel, M. L. (1999). A food web analysis of the juvenile blue crab, *Callinectes sapidus*, using stable isotopes in whole animals and individual amino acids. *Oecologia*, *120*, 416–426. https://doi.org/10.1007/s004420050874

Fogel, M. L., & Cifuentes, L. A. (1993). Isotope fractionation during primary production. In M. H. Engel & S. A. Macko (Eds.), *Organic geochemistry: Principles and applications* (pp. 73–98). Springer.

Fogel, M. L., & Tuross, N. (2003). Extending the limits of paleodietary studies of humans with compound specific carbon isotope analysis of amino acids. *Journal of Archaeological Science*, *30*, 535–545. https://doi.org/10.1016/S0305-4403(02)00199-1

Fox, M. D., Elliott Smith, E. A., Smith, J. E., & Newsome, S. D. (2019). Trophic plasticity in a common reef-building coral: Insights from $\delta^{13}C$ analysis of essential amino acids. *Functional Ecology*, *33*, 2203–2214.

Giordano, M., Beardall, J., & Raven, J. A. (2005). CO_2 concentrating mechanisms in algae: Mechanisms, environmental modulation, and evolution. *Annual Review of Plant Biology*, *56*, 99–131.

Guiry, M. D., Guiry, G. M., Morrison, L., Rindi, F., Miranda, S. V., Mathieson, A. C., Parker, B. C., Langangen, A., John, D. M., Bárbara, I., Carter, C. F., Kuipers, P., & Garbary, D. J. (2014). AlgaeBase: An on-line resource for algae. *Cryptogamie, Algologie*, *35*, 105–115. https://doi.org/10.7872/crya.v35.iss2.2014.105

Güven, K. C., Percot, A., & Sezik, E. (2010). Alkaloids in marine algae. *Marine Drugs*, *8*, 269–284. https://doi.org/10.3390/md8020269

Hare, P. E., Fogel, M. L., Stafford, T. W. Jr, Mitchell, A. D., & Hoering, T. C. (1991). The isotopic composition of carbon and nitrogen in individual amino acids isolated from modern and fossil proteins. *Journal of Archaeological Science*, *18*, 277–292. https://doi.org/10.1016/0305-4403(91)90066-X

Honya, M., Kinoshita, T., Ishikawa, M., Mori, H., & Nisizawa, K. (1993). Monthly determination of alginate, M/G ratio, mannitol, and minerals in cultivated *Laminaria japonica*. *Nippon Suisan Gakkaishi*, *59*, 295–299. https://doi.org/10.2331/suisan.59.295

Howland, M. R., Corr, L. T., Young, S. M., Jones, V., Jim, S., Van Der Merwe, N. J., Mitchell, A. D., & Evershed, R. P. (2003). Expression of the dietary isotope signal in the compound-specific $\delta^{13}C$ values of pig bone lipids and amino acids. *International Journal of Osteoarchaeology*, *13*, 54–65.

Jarman, C. L., Larsen, T., Hunt, T., Lipo, C., Solsvik, R., Wallsgrove, N., Ka'apu-Lyons, C., Close, H. G., & Popp, B. N. (2017). Diet of the prehistoric population of Rapa Nui (Easter Island, Chile) shows environmental adaptation and resilience. *American Journal of Physical Anthropology*, *164*, 343–361. https://doi.org/10.1002/ajpa.23273

Kanehisa, M., & Goto, S. (2000). KEGG: Kyoto encyclopedia of genes and genomes. *Nucleic Acids Research*, *28*, 27–30. https://doi.org/10.1093/nar/28.1.27

Kendall, I. P., Woodward, P., Clark, J. P., Styring, A. K., Hanna, J. V., & Evershed, R. P. (2019). Compound-specific $\delta^{15}N$ values express differences in amino acid metabolism in plants of varying lignin content. *Phytochemistry*, *161*, 130–138. https://doi.org/10.1016/j.phytochem.2019.01.012

Larsen, T., Bach, L. T., Salvatteci, R., Wang, Y. V., Andersen, N., Ventura, M., & McCarthy, M. D. (2015). Assessing the potential of amino acid ^{13}C patterns as a carbon source tracer in marine sediments: Effects of algal growth conditions and sedimentary diagenesis. *Biogeosciences*, *12*, 4979–4992.

Larsen, T., Taylor, D. L., Leigh, M. B., & O'Brien, D. M. (2009). Stable isotope fingerprinting: A novel method for identifying plant, fungal, or bacterial origins of amino acids. *Ecology*, *90*, 3526–3535. https://doi.org/10.1890/08-1695.1

Larsen, T., Ventura, M., Andersen, N., O'Brien, D. M., Piatkowski, U., & McCarthy, M. D. (2013). Tracing carbon sources through aquatic and terrestrial food webs using amino acid stable isotope fingerprinting. *PLoS One*, *8*, e73441. https://doi.org/10.1371/journal.pone.0073441

Larsen, T., Wooller, M. J., Fogel, M. L., & O'Brien, D. M. (2012). Can amino acid carbon isotope ratios distinguish primary producers in a mangrove ecosystem? *Rapid Communications in Mass Spectrometry*, *26*, 1541–1548. https://doi.org/10.1002/rcm.6259

Liew, J. H., Chua, K. W., Arsenault, E. R., Thorp, J. H., Suvarnaraksha, A., Amirrudin, A., & Yeo, D. C. (2019). Quantifying terrestrial carbon in freshwater food webs using amino acid isotope analysis: Case study with an endemic cavefish. *Methods in Ecology and Evolution*, *10*, 1594–1605. https://doi.org/10.1111/2041-210X.13230

Lübcker, N., Whiteman, J. P., Millar, R. P., de Bruyn, P. N., & Newsome, S. D. (2020). Fasting affects amino acid nitrogen isotope values: A new tool for identifying nitrogen balance of free-ranging mammals. *Oecologia*, *193*, 53–65. https://doi.org/10.1007/s00442-020-04645-5

Maberly, S., Raven, J., & Johnston, A. (1992). Discrimination between ^{12}C and ^{13}C by marine plants. *Oecologia*, *91*, 481–492. https://doi.org/10.1007/BF00650320

Maschek, J. A., & Baker, B. J. (2008) The chemistry of algal secondary metabolism. In C. D. Amsler (Ed.), *Algal chemical ecology* (pp. 1–24). Springer.

McMahon, K. W., Polito, M. J., Abel, S., McCarthy, M. D., & Thorrold, S. R. (2015). Carbon and nitrogen isotope fractionation of amino acids in an avian marine predator, the gentoo penguin (*Pygoscelis papua*). *Ecology and Evolution*, *5*, 1278–1290.

Miller, E. A., Lisin, S. E., Smith, C. M., & Van Houtan, K. S. (2020). Herbaria macroalgae as a proxy for historical upwelling trends in Central California. *Proceedings of the Royal Society B: Biological Sciences*, *287*, 20200732. https://doi.org/10.1098/rspb.2020.0732

Miller, R. J., & Page, H. M. (2012). Kelp as a trophic resource for marine suspension feeders: A review of isotope-based evidence. *Marine Biology*, *159*, 1391–1402. https://doi.org/10.1007/s00227-012-1929-2

Nelson, D. L., Lehninger, A. L., & Cox, M. M. (2008). *Lehninger principles of biochemistry* (Vol. 5). W.H. Freeman

Newsome, S. D., Wolf, N., Peters, J., & Fogel, M. L. (2014). Amino acid $\delta^{13}C$ analysis shows flexibility in the routing of dietary protein and lipids to the tissue of an omnivore. *American Zoologist*, *54*, 890–902.

Norris, J. N., & Fenical, W. (1982). Chemical defense in tropical marine algae. *The Atlantic Barrier Reef Ecosystem at Carrie Bow Bay Belize. I. Structure and Communities*, *12*, 417–431.

O'Leary, M. H. (1988). Carbon isotopes in photosynthesis. *BioScience*, *38*, 328–336. https://doi.org/10.2307/1310735

R Development Core Team. (2020). *R: A language and environment for statistical computing*. R Foundation for Statistical Computing.

Raven, J. A., Johnston, A. M., Kübler, J. E., Korb, R., McInroy, S. G., Handley, L. L., Scrimgeour, C. M., Walker, D. I., Beardall, J., Vanderklift, M., Fredriksen, S., & Dunton, K. H. (2002). Mechanistic interpretation of carbon isotope discrimination by marine macroalgae and seagrasses. *Functional Plant Biology*, *29*, 355–378. https://doi.org/10.1071/PP01201

Reinfelder, J. R. (2011). Carbon concentrating mechanisms in eukaryotic marine phytoplankton. *Annual Review of Marine Science*, *3*, 291–315. https://doi.org/10.1146/annurev-marine-120709-142720

Rowe, A. G., Iken, K., Blanchard, A. L., O'Brien, D. M., Døving Osvik, R., Uradnikova, M., & Wooller, M. J. (2019). Sources of primary production to Arctic bivalves identified using amino acid stable carbon isotope fingerprinting. *Isotopes in Environmental and Health Studies*, *55*, 366–384. https://doi.org/10.1080/10256016.2019.1620742

Scott, J. H., O'Brien, D. M., Emerson, D., Sun, H., McDonald, G. D., Salgado, A., & Fogel, M. L. (2006). An examination of the carbon isotope effects associated with amino acid biosynthesis. *Astrobiology*, *6*, 867–880. https://doi.org/10.1089/ast.2006.6.867

Shao, Z., Zhang, P., Lu, C., Li, S., Chen, Z., Wang, X., & Duan, D. (2019). Transcriptome sequencing of *Saccharina japonica* sporophytes during whole developmental periods reveals regulatory networks underlying alginate and mannitol biosynthesis. *BMC Genomics*, *20*, 1–15. https://doi.org/10.1186/s12864-019-6366-x

Silfer, J., Engel, M., Macko, S., & Jumeau, E. (1991). Stable carbon isotope analysis of amino acid enantiomers by conventional isotope ratio mass spectrometry and combined gas chromatography/isotope ratio mass spectrometry. *Analytical Chemistry*, *63*, 370–374. https://doi.org/10.1021/ac00004a014

Smith, R. G., & Bidwell, R. (1987). Carbonic anhydrase-dependent inorganic carbon uptake by the red macroalga, *Chondrus crispus*. *Plant Physiology*, *83*, 735–738.

Stepien, C. C., Pfister, C. A., & Wootton, J. T. (2016). Functional traits for carbon access in macrophytes. *PLoS One*, *11*, e0159062. https://doi.org/10.1371/journal.pone.0159062

Thorp, J. H., & Bowes, R. E. (2017). Carbon sources in riverine food webs: New evidence from amino acid isotope techniques. *Ecosystems*, *20*, 1029–1041. https://doi.org/10.1007/s10021-016-0091-y

Wendt, I. (1968). Fractionation of carbon isotopes and its temperature dependence in the system CO_2-gas-CO_2 in solution and HCO_3-CO_2 in solution. *Earth and Planetary Science Letters*, *4*, 64–68. https://doi.org/10.1016/0012-821X(68)90055-1

Whiteman, J. P., Elliott Smith, E. A., Besser, A. C., & Newsome, S. D. (2019). A guide to using compound-specific stable isotope analysis to study the fates of molecules in organisms and ecosystems. *Diversity*, *11*, 8. https://doi.org/10.3390/d11010008

Whiteman, J. P., Newsome, S. D., Bustamante, P., Cherel, Y., & Hobson, K. A. (2020). Quantifying capital vs. income breeding: New promise with stable isotope measurements of individual amino acids. *Journal of Animal Ecology*.

Wu, G. (2009). Amino acids: Metabolism, functions, and nutrition. *Amino Acids*, *37*, 1–17. https://doi.org/10.1007/s00726-009-0269-0

Ye, N., Zhang, X., Miao, M., Fan, X., Zheng, Y. I., Xu, D., Wang, J., Zhou, L., Wang, D., Gao, Y., Wang, Y., Shi, W., Ji, P., Li, D., Guan, Z., Shao, C., Zhuang, Z., Gao, Z., Qi, J. I., & Zhao, F. (2015). *Saccharina* genomes provide novel insight into kelp biology. *Nature Communications*, *6*, 1–11. https://doi.org/10.1038/ncomms7986

Zhang, L., Cao, Z., Liang, G., Li, X., Wu, H., & Yang, G. (2020). Comparative transcriptome analysis reveals candidate genes related to structural and storage carbohydrate biosynthesis in kelp S*accharina japonica* (Laminariales, Phaeophyceae). *Journal of Phycology*, *56*, 1168–1183.

SUPPORTING INFORMATION

Additional supporting information may be found in the online version of the article at the publisher's website.

How to cite this article: Elliott Smith, E. A., Fox, M. D., Fogel, M. L., & Newsome, S. D. (2022). Amino acid $\delta^{13}C$ fingerprints of nearshore marine autotrophs are consistent across broad spatiotemporal scales: An intercontinental isotopic dataset and likely biochemical drivers. *Functional Ecology*, 00, 1–13. https://doi.org/10.1111/1365-2435.14017